Anal. Bioanal. Electrochem., Vol. 13, No. 2, 2021, 226-238

Analytical & Bioanalytical Electrochemistry

2021 by CEE
www.abechem.com

Full Paper

Development of a New Sensitive Electrochemical Sensor for Dapsone Detection using a Cobalt Metal-Organic Framework/Molecularly Imprinted Polymer Nanostructures

Maryam Malekzadeh,[1] Alireza Mohadesi,[1,*] Mohammad Ali Karimi,[1] and Mehdi Ranjbar[2,*]

[1]Department of Chemistry, Payame Noor University, P.O. Box 19395-4697, Tehran, Iran
[2]Neuroscience Research Center, Institute of Neuropharmacology, Kerman University of Medical Sciences, Kerman, Iran

*Corresponding Author, Tel.: +98-34-31325241; Fax: +98-34-31325003

E-Mails: Mohadesi_a@yahoo.com (Alireza Mohadesi); Mehdi.Ranjbar@kmu.ac.ir (Mehdi Ranjbar)

Received: 24 January 2021 / Received in revised form: 19 July 2021 / Accepted: 31 July 2021 / Published online: 30 September 2021

Abstract- This study reports a novel, inexpensive, and efficient approach for the synthesis of the Co metal-organic framework molecularly imprinted polymer nanoparticles (Co-MOF/MIP), which can be used as a highly selective and sensitive method for the determination of dapsone (DDS). MOFs due to high potential in the presence of porosity properties can be used in sensors based on glassy carbon electrode (GCE). The synergistic effect of the porosity network structure on glassy carbon electrode increases the power of the limits of detection (LOD). Average size of the MOFs was obtained about 17- 27nm. The first metal-organic frameworks (MOFs) with high specific surface area and high porosity were synthesized by morcellation and microwave methods. Some parameters affecting the sensor response were optimized, and a calibration curve was plotted using the differential pulse voltammetric (DPV) technique. The calibration curve of dapsone was linear in the concentration range of 0.5 up to 170 µM with y=0.0259x+0.4887 and R^2= 0.998. The linear response was obtained in the range of 0.5-170 µM of DDS concentrations with a detection limit of 0.15 µM under optimized conditions. Also, the relative standard deviation (RSD) was calculated as 1.42 % for five electrodes prepared independently.

Keywords- Dapsone; Molecularly imprinted polymers; Metal-organic framework; Electrochemical sensor

1. INTRODUCTION

Sulphone dapsone (4,4-diaminodiphenylsulphone, DDS) [1] has been used as an oral drug since 1949. It was initially approved for leprosy [2], for which it is still frequently used. In addition to its antimicrobial effects, dapsone is a potent anti-inflammatory agent with strong effectiveness for dermatitis herpetiformis and a wide variety of other inflammatory dermatological conditions. It has also been used for the treatment of acne and various other skin conditions [3]. Numerous methods adopted for the quantification of dapsone are spectrophotometry [4], liquid chromatography (LC) [5], high-performance liquid chromatography (HPLC) [4-7], and polarography [8]. In this paper, it is shown that MIPs serve as synthetic receptors for a wide variety of molecules and are synthesized using molecular imprinting techniques. Molecular imprinting involves the use of functional monomers and template molecules to create specific and selective cavities in a polymer matrix [9,10]. Polymerization is performed in the presence of template molecules, represented by the analyte of interest. These materials are somewhat similar to biological specific receptors with respect to their high selectivity for the target molecule and their recognition mechanism [11]. It is reported that the affinity between the MIP's receptors and template molecules has a significant effect on the sensor's sensitivity, and this affinity is inversely proportional to the MIP's particle size [12]. Some examples of electrochemical sensors based on imprinted polymers include impedance measurement [13], field-effect transistor [14], capacitance [15], conductometric [16], amperometric [17,18], and voltammetric [19-24] methods. Therefore, the synthesis of nanosized MIP particles is desirable for improving the sensitivity of the sensor.

Metal-organic frameworks (MOFs) are metal complexes with organic linkers, such as carboxylates or phosphonates, that were first defined by Yaghi et al. in 1995 [25,26]. MOFs have attracted increasing interest in recent years as highly sensitive platforms for the development of sensors [27,28]. The use of MOFs is extensive due to their numerous architectural properties, including a stable framework, high porosity, large internal surface area, pore volume, a wide range of thermal and chemical stability, and non-toxic nature. They have been of interest owing to their promising application in various research and industrial areas such as gas separation/storage [29,30], magnet [31], sensing [32], heterogeneous catalysis [33], and pseudo-capacitors [34-36]. In previous work, an anti-electrochemical sensor based on iron oxide nanoparticles was fabricated to detect dapsone using a molecular imprinted polymer. Molecular imprinted polymer (MIP) synthesized in the presence of polymerization of functional monomers in the presence of template compounds, which results in the creation of a three-dimensional matrix with specific identification. After polymerization, the pattern molecule leaves the polymer matrix and leaves cavities that do not conflict with the pattern in size, position, and shape selection [37,38]. As an emerging research topic, hybrid molecularly imprinted polymers are developed by combining the benefits of MOF and MIPs, opening paths for the development of a new generation of sensors. For this purpose, an electrochemical sensor

based on bare GCE modified with MIP and CO-MOF nanostructures was prepared by electropolymerization and employed for the determination of dapsone in pharmaceutical samples.

2. EXPERIMENTAL PROCEDURE

2.1. Materials and apparatus

Materials of the analytical grade and doubly distilled water were used. Dapsone ($C_{12}H_{12}N_2O_2S$, MW: 248.30 $g \cdot mol^{-1}$, 99%, 4-aminobenzoic acid ($C_7H_7NO_2$, MW:137.14 g/mol, 99%), sodium sulfate (Na_2SO_4, MW:142.04 g/mol, CAS, 7757-82-6, 99%), potassium ferrocyanide ($K_3[Fe(CN)_6]$, MW:329.24, 99%, sulfuric acid (Na_2SO_4, CAS:7757-82-6, 99%), ethanol (CH_3CH_2OH, Molar mass: 46.07 g/mol, Density: 789 kg/m^3, 99%), sodium hydroxide (NaOH, Molar mass: 39.997 g/mol, Density: 2.13 g/cm^3, 96%) and other reagents were purchased from Merck (Darmstadt, Germany). A pH meter (Metrohm, Model 827, Switzerland) was utilized for pH adjustments. Electrochemical data were obtained with a polarograph connected to a personal computer (PC) via a USB port and in NOVA 2.2 software (Metrohm, Model 797 VA computrance, Switzerland), using a three-electrode system consisting of modified GCE (2 mm), Ag/AgCl (sat. KCl), and platinum wire were used as a working electrode, reference electrode, and counter electrode, respectively. All the measurements were made at room temperature. The surface morphology of the modified electrodes was characterized by a scanning electron microscope (SEM) (JEOL JSM-6700F, Japan).

2.2. Synthesis of MOF Nanostructures

To prepare the Co-MOF nanostructures, in a typical procedure, 0.25 g of $Co(OAc)_2.4H_2O$ was dissolved in 30 ml of distilled water (DW) under 400 rpm at 50 ◦C with magnetic stirring for 2 h; then, 0.3 g [2,6]-pyridinedicarboxylic acid was added dropwise to the above solution, and pH was adjusted on 7.5 with NaOH 2M. The suspension content was placed under an ultrasonic probe (60 W (18 KHz)) with a period cycle including 3 s on the pulse and 1 s of silence for 15 min. In another beaker, 0.005 g of cetyltrimethyl ammonium bromide (CTAB) was dissolved in 10 ml of DW; after observing the foam bubbles on the solution, it was added to the main solution under stirring at 400 rpm and 50 °C for 45 min, and the pH of the solution was simultaneously adjusted to 7.5 using NaOH. The as-synthesized Co-MOF nanostructures were centrifuged and washed with DW and extra ethanol twice.

2.3. Preparation of the Co-MOF/MIP electrode

Prior to electropolymerization, the surface of the GCE (glassy carbon electrode) was polished with alumina slurry and rinsed with DW. Then, it was cleaned by sonication in DW and absolute ethanol for 3 min. For the modification of the GCE, it was immersed in phosphate-

buffered saline (PBS) (0.2 M, pH=6.5) and 1.0 mg of the prepared MOFs. After deoxygenating the reaction solution by bubbling nitrogen gas for about 5 min, and scanning for several cycles using cyclic voltammetry (CV) from -0.5 V to 1.5 V at 50 mV s^{-1} under stirring until a stable voltammogram was observed. The DDS-imprinted film and non-imprinted film were prepared via the electropolymerization method. First, 5.0 mM pABA (as a functional monomer) and 1.0 mM dapsone (as a template) in the PBS buffer (0.2 M, pH=6.5) as the supporting electrolyte template were electrodeposited on the surface of the Co-MOF/MIP/GCE electrode by employing CV in the potential range of -0.6 V to 1.0 V at a scan rate of 50 mVs^{-1} for 15 cycles. Subsequently, the polymer film was immersed in 1:2 (v/v) acetic acid-methanol solution for 30 seconds to remove DDS from the polymeric matrix. For comparison, the non-molecularly imprinted polymer (Co-MOF/NIP/GCE) was prepared under the same conditions in the absence of DDS.

2.4. Experimental measurement procedures

The electrochemical characterization of the modified electrodes and the bare electrode was performed using CV. The cyclic voltammogram was recorded between -0.6 V and 1.0 V at a scan rate of 50 mV/s. The optimization of experimental conditions, calibration curve, selectivity, and sample analysis was performed using differential pulse voltammetry (DPV). DPV was performed from -0.6 V to 1.0 V, the pulse amplitude was 50 mV, and the pulse time was 0.04 s. After each experimental run, the electrode was immersed for 15 scans in the range of -0.5 to 1.5 at 50 mVs^{-1} in sodium sulfate (0.2 mol L^{-1}) to remove the template in order to reuse the electrode. All the experiments were conducted at room temperature.

3. RESULTS AND DISCUSSION

3.1. Structural and morphological characterization

Fig. 1a displays the XRD pattern of Co-MOF nanostructures. The crystalline plates are well-formed and the sample has high crystallinity. The size of the NPs is in good agreement with the microscopic images and is calculated by the Debye-Scherrer equation by calculating the width cycle at half maximum at ~50 nm. The characterization of the synthesized Co-MOF nanostructures was performed by means of SEM and XRD. The SEM image of the prepared nanoparticles (NPs) shows a homogeneous globular structure with an average diameter of 110 nm (Fig. 1b).

A significant peak in region 3423 cm^{-1} is related to the ∂(OH) stretching in [2,6]-pyridinedicarboxylic acid. The peaks at 2856 cm^{-1} confirm the presence of CH_3, CH_2, and CH bonds in the final structure groups in the Co-MOF nanostructures. Also, the stretch vibrations of C=O groups appear at 1474 cm^{-1} and are related to organic ligand structures. Intense peaks in the wavelength region of ~1430 cm^{-1} are related to C-N of [2,6]-pyridinedicarboxylic acid. A few peaks in the area 1118 cm^{-1} are related to the C–O bonds of the Co-MOF nanostructures.

Peaks observed in the 1000 cm^{-1} area are related to Co-CH and Co in the final Co-MOF nanostructures. The FT-IR spectrum of Co-MOF nanostructures is shown in Fig. 2.

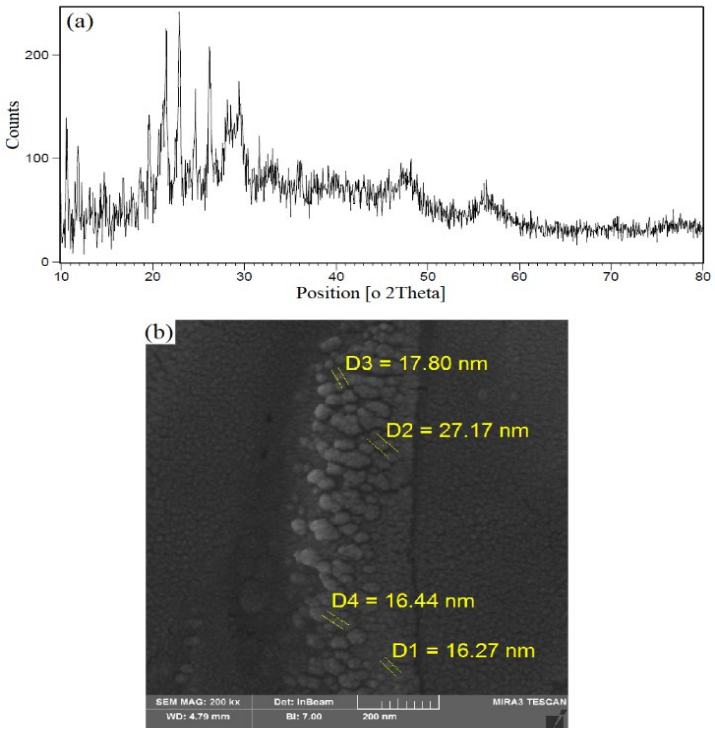

Fig. 1. XRD pattern (A) SEM images (B) of Co-MOF nanostructures

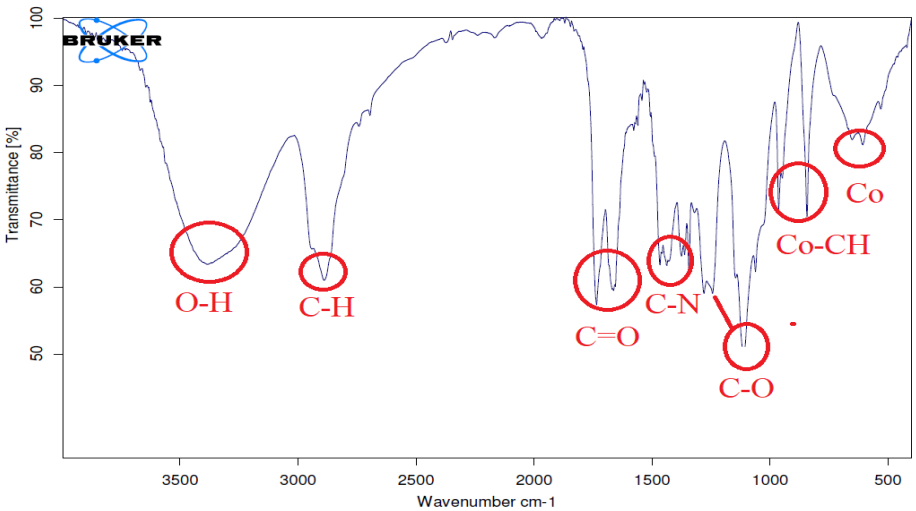

Fig. 2. FT-IR spectrum of Co-MOF nanostructures

3.2. Electrochemical behavior of the modified sensor

To investigate the electrochemical behavior of pABA after 15 CVs in the phosphate buffer solution (pH 7; 0.1 M) between -0.5 and +1.5 V on the GCE surface was used. Dapsone

molecules were extracted from the Co-/MOF/MIP by placing the electrode in 0.2M Na_2SO_4 solution (pH 6.5) and electrochemical scanning between -0.6 and 1.0 V using CV. A DPV with a deposition potential of 1.0 V, deposition time of 90 s in 0.2M Na_2SO_4 solution, and different concentrations of dapsone were applied to rebind dapsone to the Co-/MOF/MIP film. The non-imprinted polymer (NIP) was prepared using the same process in the absence of dapsone molecules on the electrode surface, and was used to verify the method in the presence of potassium ferrocyanide as a probe all measurements were accomplished. Fig. 3 shows the voltammogram of the potassium ferrocyanide solution attached to the Co/MOF/NIP and Co/MOF/MIP electrodes in the presence and absence of dapsone which are electrochemically committed on the GC electrodes. When the Co/MOF/ MIP film modified onto the GCE surface, it was investigated with a potassium ferrocyanide probe (Fig. 3A), and no peak is observed (Curve a). the potassium ferrocyanide anions cannot contact the surface electrode because the MIP film is sufficiently compressed. However, the ferrocyanide can be obtained at the electrode surface through the cavity sites, which are created after the MIP fibers at the surface of the Co-MOF/MIP/GCE and the oxidation/reduction peak of ferrocyanide (curve b). Finally, by plunging the Co-MOF/MIP/GCE in the dapsone solution at a deposition potential of 1.0 V for 90 s, the probe current response was decreased (Curve c). Fig. 3B shows that compared to the ferrocyanide probe, the polymer synthesized in the absence of dapsone (NIP) has a different behavior compared to the Co-MOF/MIP, the situation for removing the dapsone from this electrode has no effect. The behavior of the Co-MOF/MIP electrode compared to the Co-MOF/NIP electrode indicates that the Co-MOF/MIP electrode provides suitable conditions for the electrochemical measurement of dapsone.

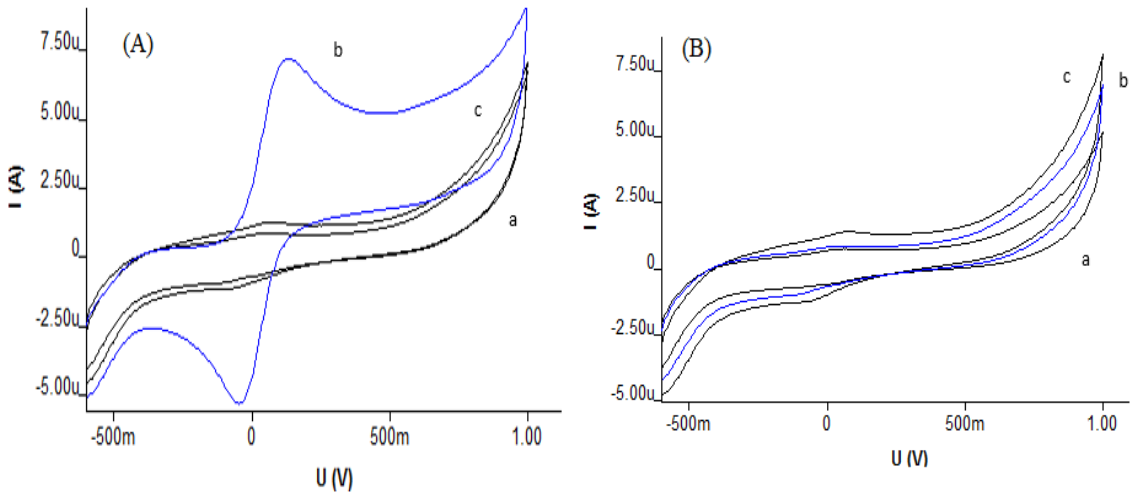

Fig. 3. (A) The cyclic voltammogram (50 mVs−1) of Co-MOF /MIP/GCE, and (B) Co-MOF /NIP/GCE in 0.2 M Na_2SO_4 solution containing 0.2 mM [K4[Fe $(CN)_6$]] under various conditions: after (a) synthesis, (b) dapsone removal and (c) dapsone rebinding

3.3. Optimization of experimental conditions

3.3.1. Effect of dapsone concentration

To achieve the best separation efficiency, the concentration of the dapsone was optimized. Moreover, in the pre-electropolymerization mixture, the identification and quantification of the MIP sites show a direct role in the mechanisms of pABA-dapsone interactions.

By increasing the concentration of dapsone up to 1 mM, the sensor response was reduced in proportion to the concentration of dapsone, and the Co-MOF/MIP deposited on GCE became more engaged with the template. Fig. 4A illustrates the effect of dapsone concentration on the Co-MOF/MIP electrode response.

3.3.2. Monomer concentration effect

The influence of the monomer concentration on the behavior of the Co-MOF/MIP sensor during the Co-MOF/MIP electropolymerization was intended. The films were synthesized in solutions of different amounts of pABA and a constant concentration of dapsone for determining the effect of [pABA] on the response of the Co-MOF/MIP, ranging from 1 mM to 10 mM. Fig. 4B shows that the best monomer concentration is attained at 5 mM.

3.3.3. Effect of pH

The effect of pH solution on the performance of the modified electrode toward dapsone was studied by CV in the pH range of 2 to 11, and Fig. 3C presents the results. The peak current increases with pH rising up to 6.5, and then is decreased with further increasing the pH. Hence, pH of the phosphate buffer solution was chosen as the optimal pH value in the following experiments.

3.3.4. Effect of polymerization cycle

The sensitivity of the electrochemical sensor depends on the synthesis procedure of the Co-MOF/MIP film. The cycle number for the electrodeposition during CV has a significant effect on the imprinted polymer. The optimization of the cycle number was investigated in 5, 8, 10, 15, and 20 cycles (Fig. 3D). The peak current reaches a maximum with 15 cycles, and then decreases if the number of cycles of polymerization is <20. The polymer membranes became fine and fewer imprinting sites are formed on the surface of the electrode, which may reduce sensitivity. At higher cycle numbers, the template molecule located in the central region of the film cannot be completely taken out from the polymer matrix; It can be concluded that the formation of thicker films might have resulted in reduced number of accessible printed sites in the Co-MOF/MIP film. Therefore, 15 cycles were used as the optimum number of scan cycles during electropolymerization.

3.3.5. Effect of -template removal

After electrosynthesis, the template must be removed in order to format the imprinting cavities. There is electrostatic and hydrogen bonding between the amino, sulfonyl, and hydroxyl groups in both 4-aminobenzoic acid monomer and dapsone templates. Extraction with a solvent is the most ordinary method, and a solvent can strongly interact with the polymer and be used for template cleaning. In this work, pure water, methanol-acetic acid (1:2, V/V), alcohol, acetic acid, and water solution (1:1, V/V) were each used to remove the template. It was found that, by the electropolymerization method, the MIP sensor is immersed for 15 scans in the range of -0.5 to 1.5 at $50mVs^{-1}$ in sodium sulfate ($0.2\ molL^{-1}$) to remove the imprinting molecules. Therefore, the imprinting electrode in sodium sulfate completely removed the template, which was verified electrochemically.

Effects of the potential and time for rebinding of dapsone on the modified electrode

The influence of potential on the anodic peak current for rebinding of dapsone on Co-MOF/MIP/GCE was studied by varying the potential from 0.2 to 1.4 V vs. the reference electrode. By immersing the MIP-modified electrode in the template solution under different conditions such as phosphate buffer solution with pH=6.5 and dapsone (1.0 mM), after removing the template from the Co-MOF/MIP/GCE film, the different potential and times were investigated for rebinding of the template molecule. The dissociation times from 10 to 120 s were evaluated (Fig. 4E). Thus, the accumulation time of 90 s was chosen for further experiments, and 1.0 V was used as an optimum potential for all subsequent measurements (Fig. 4F).

3.3.6. Performance of the imprinted sensor

The differential pulse voltammogram (DPV) signals obtained for the different concentrations of dapsone, as well as the plotted calibration curves are shown in Fig. 5. The calibration graph obtained for dapsone determination depicts a linear relationship over dapsone concentration in the range of 0.5 μM to 170 μM. When the concentration is larger than the ceiling limit, the peak currents do not significantly increase, which may be due to the occupation of all cavities presented in the imprinted polymers. The linear regression equation is: I_P (μA) = 0.0259 C + 0.4887 dapsone (μM) (R^2 = 0.9983).

The limits of detection (LOD) and quantitation (LOQ) were calculated using the relation ks/m, where k=3 for LOD and 10 for LOQ, s represents the standard deviation of the peak current of the blank, and m indicates the slope of the calibration curve for dapsone. The LOD and LOQ values are found to be 0.15 and 0.5 μM, respectively, indicating the sensitivity of the proposed method.

To confirm the efficiency of the designed sensor, the effects of some compounds with similar structures or groups to dapsone were experimented. Substance is present the change of the peak current of the dapsone in electrochemical sensing. Effects of disturbing species on the

detection of 30 mM the dapsone from solutions with a 10 times concentration of various additives used as excipients in 0.2 M Na_2SO_4 solution containing 0.2 mM [K_4[Fe (CN)$_6$]] as supporting electrolyte shown in (Table 1), which fit the shape, size and functional groups of pABA during the polymerization process.

To check the reproducibility of the prepared electrode, under the same experimental conditions, five Co-MOF/MIP/GCE sensors were fabricated independently. The relative standard deviation (RSD) 1.42% is obtained, showing that the precision of the results is satisfactory. In addition, the RSD of the same sensor for eight successive assays is 1.43%. The storage stability of the sensor was also investigated. It was determined that the sensor can retain >90% of its original response after being used at least 60 times or stored in a refrigerator for two months. The results demonstrate that the sensor possesses excellent repeatability and stability.

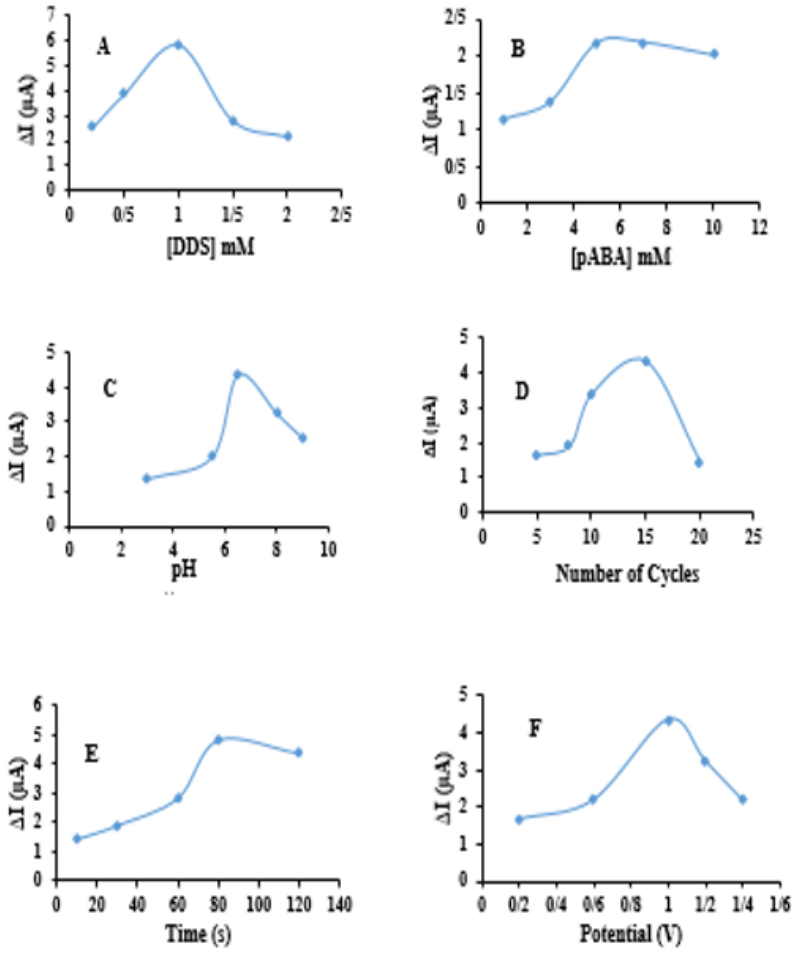

Fig. 4. Optimization of analytical conditions affecting the Co-MOF/MIP/GCE film; effect of: (A) dapsone, and (B) pABA concentrations(C) pH value (D) polymerization cycle (E) the potential for rebinding (F) time for rebinding of dapsone on the modified electrode

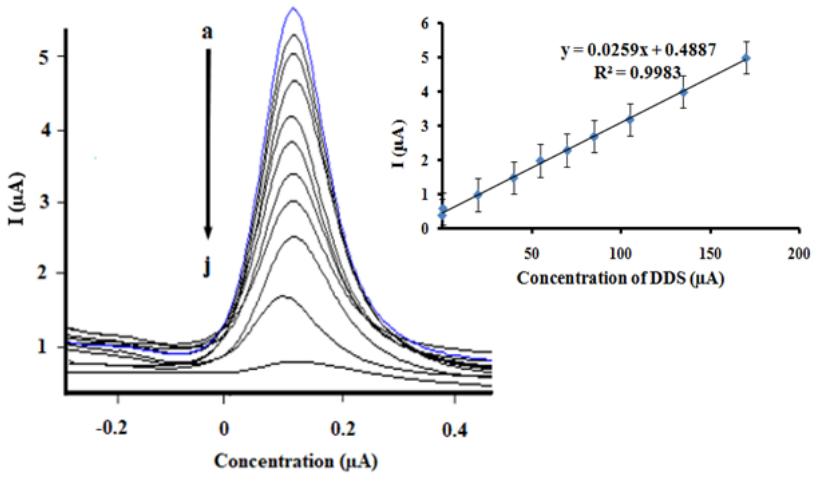

Fig. 5. Differential pulse voltammetry of the Co-MOF/MIP/GCE in various concentrations of the dapsone solution, a to j: 0, 0.5, 20, 40, 55, 70, 85, 105, 135 and 170 µM, and the related calibration curve

Table 1. Effects of disturbing species on the detection of 30 mM the dapsone from solutions with a 10 times concentration of various additives used as excipients in 0.2 M Na_2SO_4 solution containing 0.2 mM [K_4[Fe (CN)$_6$]] as supporting electrolyte.

Additive	Recovery, % (n = 3)
Nicotinamide	104.0 (±0.8)
Nicotinic acid	102.1 (±1.1)
Ascorbic acid	105.1 (±1.2)
Thiamine hydrochloride	100.2 (±1.3)
Calcium pantothenate	102.4 (±1.2)
Pyridoxine hydrochloride	99.5(±1.4)
Riboflavin	100.9 (±2.0)
Streptomycin sulphate	104.0 (±1.2)

3.4. Application of the method for a real sample

The performance of the proposed sensor was examined to determine dapsone in the prepared solutions containing aliquot amounts of dapsone (spiked in the solutions) (n=5). Table 2 summarizes the results. The recovery of dapsone is found to be between 96% and 102% using the DPV method. Also, the RSD of the proposed method is <0.014%, which indicates the acceptable precision of the voltammetry determination of dapsone using the modified electrode. The results confirm that the proposed Co-MOF/MIP sensor can be successfully applied for the determination of DDS in real samples.

Table 2. Recovery data for detection of DDS in gel sample using CO-MOF/MIP/GCE in 0.2 M Na_2SO_4 solution containing 0.2 mM [K_4[Fe (CN)$_6$]] as supporting electrolyte.

gel sample	DDS added (μM)	Average of DDS found (μM)	SD	Recovery (%)	RSD (%)
1	20	20	0.0024	100	0.02
2	49	50	0.0002	102	0.014
3	80	76	0.0016	96	0.06
4	100	97	0.0021	97	0.07

Table 3. Comparison of Co-MOF/MIP/GCE sensor with other reported methods for the determination of the dapsone.

Method	Linear range (μM)	Detection limit (μM)	Recovery (%)	RSD (%)	Reference
Stationary GCE	-	0.0036	98.8-99.3	0.4	[39]
CPE GCE	1.0-499.4, 49.9-299.6	31.7	101	<1.46	[40]
MIP–CL	1.0−100.0	5.27×10^{-7}	98.8-105	1.8	[41]
MIP/GCE	1.0-110.0	3×10^{-7}	95.55-102	1.4	[40]
MIP/GCE/Co-MOF	0.5-170.0	1.5×10^{-7}	96-102	1.42	This work

4. CONCLUSION

The application of a novel hybrid electrochemical sensor with the MIP film of improved surface area using Co-MOFs nanostructures was demonstrated for determining the DDS. In comparison to other DDS electrochemical sensors that have been reported, the proposed sensor had an acceptable limit of detection (Table 3). Initially, the thin layer coating of Co-MOFs and molecularly imprinted polymer were deposited on the surface of the glass carbon electrode for the preparation of the sensor. The relative standard deviation (RSD) was calculated as 1.42 %. This sensor seems to be promising for the determination of DDS with many desirable properties, including a simple fabrication procedure, high stability, good reproducibility and

repeatability, high sensitivity, and fast response time. Thus, investigations are currently being conducted on nano-structuration for enhancing the sensitivity of these sensors and increasing the number of accessible cavities. The method presented an acceptable specificity for dapsone in a pharmaceutical sample.

REFERENCES

[1] W. Foye and T. Lemke, Lippincott Williams and Wilkins (2008) Philadelphiap.
[2] Z. Zhang, The Journal of organic chemistry 84 (2019) 3919.
[3] Y. I. Zhu and M. J. Stiller, Journal of the American Academy of dermatology 45 (2001) 420.
[4] P. Nagaraja, Indian journal of pharmaceutical sciences 65 (2003) 82.
[5] M. S. Seehra, S. Ranganathan and A. Manivannan, Anal. Lett. 41 (2008) 2162.
[6] M. Homma, Journal of pharmaceutical and biomedical analysis 23 (2000) 629.
[7] R. Hollanders, Journal of Chromatography B: Biomedical Sciences and Applications 744 (2000) 65.
[8] H. Oelschläger and G. Modrack, Archiv der Pharmazie 319 (1986) 10.
[9] T. Guo and Y. Li, Biomaterials 26 (2005) 5745.
[10] L. Qin, Journal of Chromatography A 121 (2009) 807.
[11] H. Bloemhof, B. Greijdanus and D. Uges, Ziekenhuisfarmacie 11 (1995) 38.
[12] T. Alizadeh, Analytica chimica acta 623 (2008) 101.
[13] R. Suedee, W. Intakong and F. L. Dickert, Analytica chimica acta 569 (2006) 66.
[14] C. H. Weng, Sens. Actuators B 121 (2007) 576.
[15] D. Kriz and K. Mosbach, Anal. Chim. Acta 300 (1995) 71.
[16] A. Gómez-Caballero, Electroanalysis 19 (2007) 356.
[17] T. Alizadeh, Food Chem. 130 (2012) 1108.
[18] M. Blanco-Lopez, Biosens. Bioelectron. 18 **(**2003) 353.
[19] T. Alizadeh, M. R. Ganjali and M. Akhoundian, Int. J. Electrochem. Sci. 7 (2012) 10427.
[20] T. Alizadeh, Biosens. Bioelectron. 25 (2010) 1166.
[21] T. Alizadeh, Talanta 79 (2009) 1197.
[22] L. Chen, S. Xu and J. Li, Chem. Soc. Rev. 40 (2011) 2922.
[23] G. Vasapollo, Int. J. Mol. Sci. 12 (2011) 5908.
[24] J. García-Calzón, M. Díaz-García, Sens. Actuators B 123 (2007) 1180.
[25] H. Zhou, J. R. Long and O. M. Yaghi, Chem. Rev. 12 (2012) 234.
[26] K. J. Gagnon, H. P. Perry and A. Clearfield, Chem. Rev. 122 (2012)1034.
[27] K. N. Chappanda, Sens. Actuators B 257 (2018) 609.
[28] M. Saraf, R. Rajak and S. M. Mobin, J. Mater. Chem. A 4 (2016) 16432.
[29] B. Wang, Green Energy & Environment 3 (2018) 191.
[30] D. Farrusseng, John Wiley & Sons 345 (2011) 566.

[31] T. Storr, Polyhedron 108 (2016) 80.
[32] X. Zhu, Chem. Commun. 49 (2013) 1276.
[33] I. Luz and F. L. Xamena, J. Catal. 276 (2010) 134.
[34] F. B. Ajdari, A. Kowsari and A. Ehsani, J. Colloid Interface Sci. 509 (2018) 189.
[35] M. Naseri, J. Colloid Inter. Sci. 484 (2016) 314.
[36] F. B. Ajdari, E. Kowsari and A. Ehsani, J. Solid State Chem. 2 (2018) 155.
[37] A. Afkhami, F. Gomar and T. Madrakian, J. Electrochem. Soc. 162 (2015) 109.
[38] W. Alia, C. Queiroz and C. M. Brett, Sens. Actuators B 325 (2020) 1287.
[39] R. Sane, Drugs 19 (1982) 198.
[40] A. Afkhami, F. Gomar and T. Madrakian, J. Electrochem. Soc. 162 (2015) 109.
[41] F. Lu, Anal. Bioanal. Chem. 404 (2012) 79.